Supporting information

Electrochemical Exfoliation of Ultrathin Ternary Molybdenum Sulfoselenide Nanosheets to Boost Energy-efficient Hydrogen Evolution Reaction

Jincheng Si,[a,b] Hanlin Chen,[a] Chaojun Lei,[a] Yange Suo,[b,*] Bin Yang,[a] Zhiguo Zhang,[b] Zhongjian Li,[a] Lecheng Lei,[a] Junhong Chen,[c] Yang Hou,[a,d,e*]

[a] Key Laboratory of Biomass Chemical Engineering of Ministry of Education, College of Chemical and Biological Engineering, Zhejiang University, Hangzhou 310027, China

[b] Department of Energy and Environmental Systems Engineering, Zhejiang University of Science and Technology, Liuhe Road 318#, Hangzhou, Zhejiang Province 310023, China

[c] Department of Mechanical Engineering, University of Wisconsin-Milwaukee, Milwaukee, WI, 53211 USA

[d] Institute of Zhejiang University - Quzhou, 78 Jiuhua Boulevard North, Quzhou 324000, China

[e] Ningbo Research Institute, Zhejiang University, Ningbo 315100, China

Experimental section

Synthesis of bulk $MoSe_xS_{2-x}$

The bulk $MoSe_xS_{2-x}$ was synthesized by a traditional solid phase synthesis method. First, 0.95 g of Mo powder (Alfa Aesar, 99%), 0.78 g of Se powder (Alfa Aesar, 99%) and 0.96 g of S powder (Alfa Aesar, 99%) were mixed together and ground at the same time. Then, powder mixture was sealed in a vacuum quartz tube and placed in a tube furnace. The temperature of tube furnace was increased from 20 ℃ to 950 ℃ within 2 h, and then remained the temperature for 60 h. The bulk $MoSe_xS_{2-x}$ was successfully synthesized when cooled to room temperature.

Synthesis of ternary $MoSe_xS_{2-x}$ nanosheets

The bulk $MoSe_xS_{2-x}$ was synthesized by a traditional solid phase synthesis method. Then, the bulk $MoSe_xS_{2-x}$ was fixed on the copper sheets using conductive silver paint. The bulk $MoSe_xS_{2-x}$ was directly installed on the clamp of the cathode with Pt plate as negative pole in Tetrabutyl ammonium bromide (TBAB) acetonitrile solution (10 mg mL^{-1}). When applying a moderate potential of -3.0 V for 30 min, the ternary $MoSe_xS_{2-x}$ nanosheets was dispersed in the electrolyte. Further, the ternary $MoSe_xS_{2-x}$ nanosheets were filtered and mixed with the N-Methyl-2-pyrrolidone (NMP) solution for 1 h mild sonication. The ternary $MoSe_xS_{2-x}$ nanosheets were obtained through 10,000 rpm of centrifugation, followed by a freeze-dried treatment.

Characterization

X-ray diffraction (XRD) was conducted on a RIGAKU D/MAX 2550/PC X-ray diffractometer with Cu Kα radiation. Scanning electron microscopy (SEM) micrographs were achieved on a field emission scanning electron microscopy (FESEM), Supra 55 microscope. Raman data were collected on Laser Confocal Raman Microspectroscopy (LabRAM HR Evolution, wavelength = 532 nm). X-ray photoelectron spectroscopy (XPS) was performed on Thermo Fisher Scientific, Escalab 250Xi with Al Ka radiation. Atomic force microscopy (AFM MultiMode VEECO America with tapping Mode) was used to measure the thickness of the materials. The structure and morphology of all testing materials were investigated by transmission electron microscopy (TEM, HT7700) and high-resolution TEM

(HRTEM, JEM-2100, 200 kV).

Electrochemical tests

Electrochemical measurements were conducted on an electrochemical analyzer (CHI 760E), in which a glassy carbon electrode (3 mm in diameter, 0.07 cm^2) with catalyst acted as the working electrode, an Ag/AgCl electrode used as the reference electrode, and a graphite rod used as the counter electrode. The electrolyte solution was 1.0 M KOH. The dispersions of catalysts were achieved by 5 mg of catalyst and 5 mg of carbon black with 50 μL of Nafion solution (5 wt.%) dispersed in 450 μL of ethanol to form a homogeneous ink with sonication for 2 h. Next, the homogeneous ink was loaded onto the glassy carbon electrode with a loading amount of 0.285 mg cm^{-2}. In order to facilitate easier integration of the electrode into devices for practical applications, the ternary $MoSe_xS_{2-x}$ nanosheets were further drop-casted onto Ni foam with a loading capacity of 0.285 mg cm^{-2} as cathode for HER. All polarization curves were presented with iR correction. The electrochemical impedance spectroscopy (EIS) measurements on catalysts were performed at a potential of -0.21 V (vs. RHE). The electrochemically active surface area (ECSA) of catalysts was evaluated by cyclic voltammogram (CV) cycling from 0.09 to 0.21 V (vs. RHE) in 1.0 M KOH at sweep rates of 20-100 mV s^{-1}.

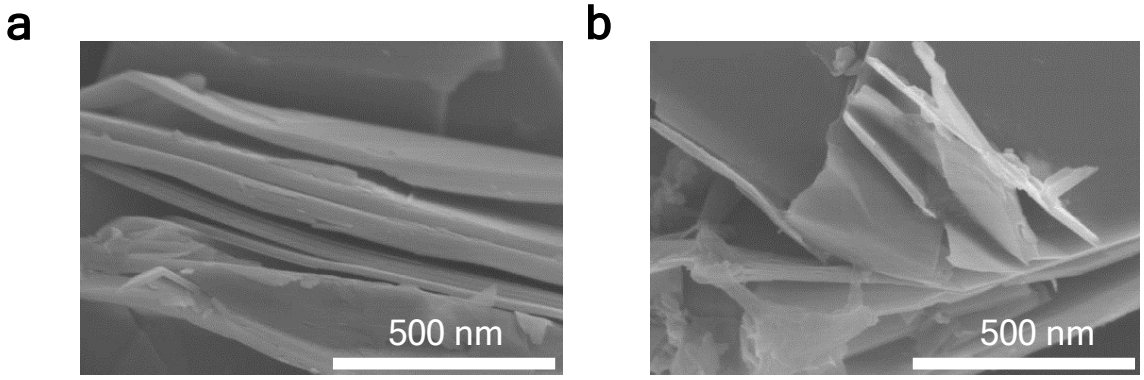

Figure S1. (a-b) FESEM images of bulk $MoSe_xS_{2-x}$ after 10 and 20 min exfoliations.

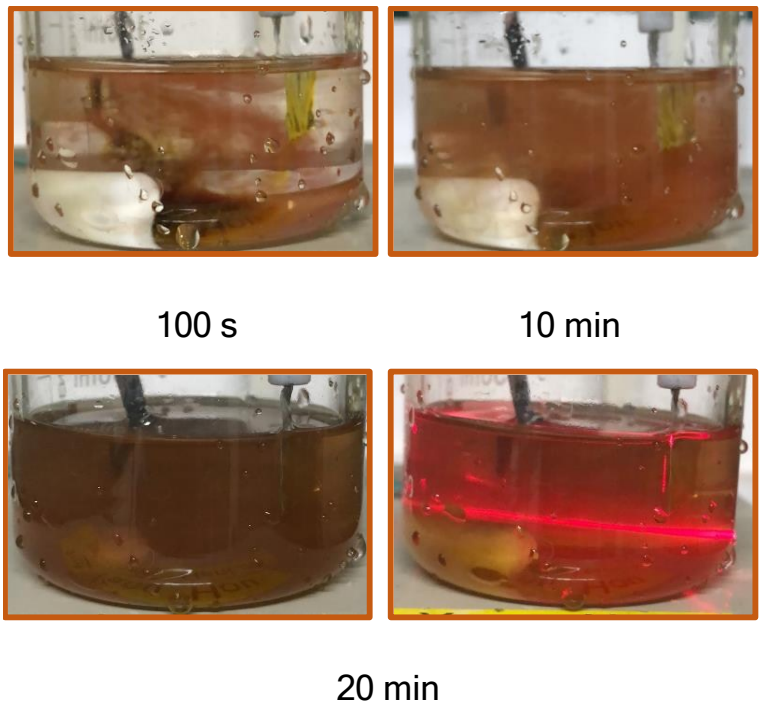

Figure S2. Digital photos of exfoliating processes over time.

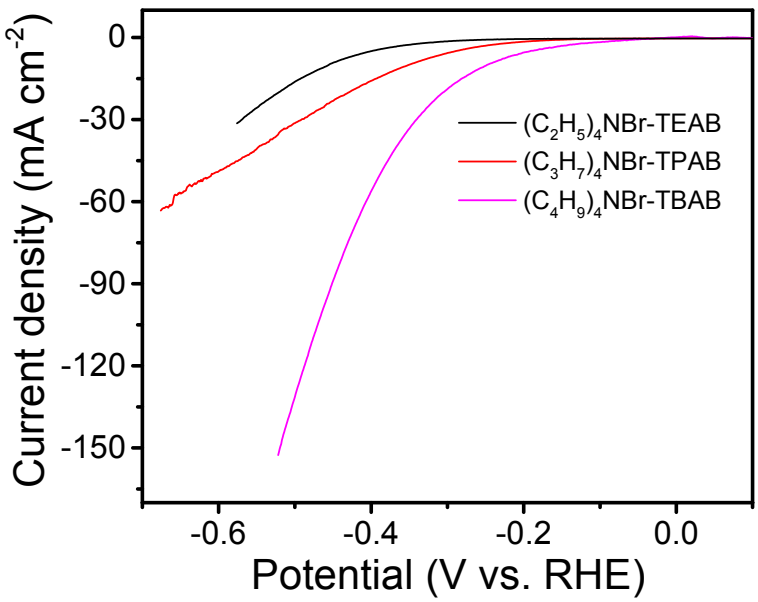

Figure S3. Polarization curves of ternary $MoSe_xS_{2-x}$ nanosheets obtained by electrochemical exfoliating with different electrolytes.

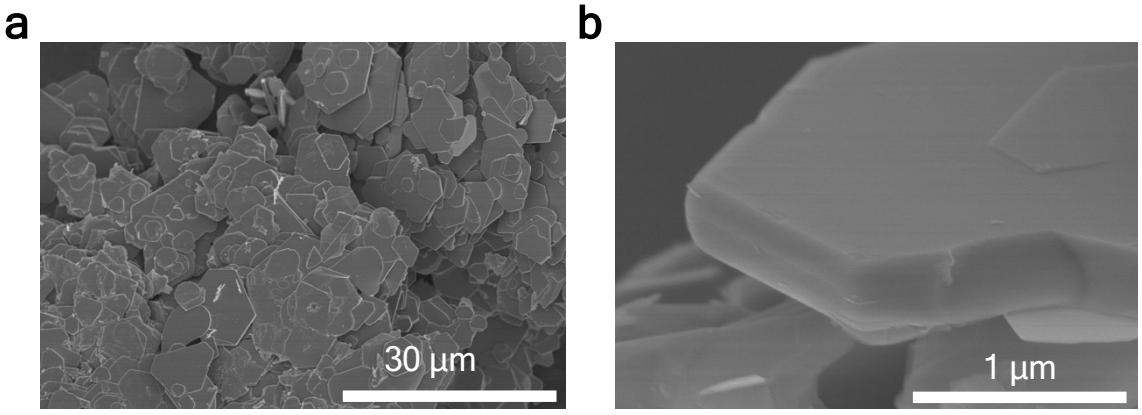

Figure S4. (a-b) FESEM images of bulk $MoSe_xS_{2-x}$ with different magnifications.

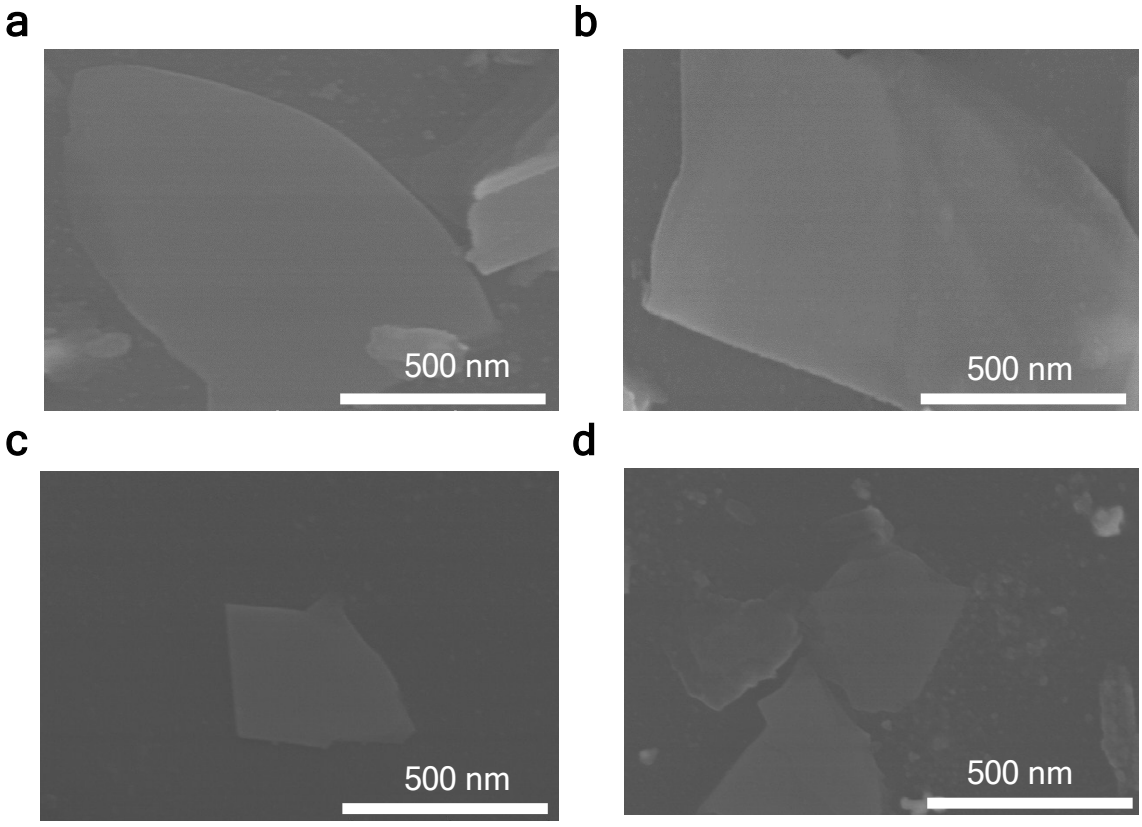

Figure S5. FESEM images of ternary $MoSe_xS_{2-x}$ nanosheets with different magnification levels.

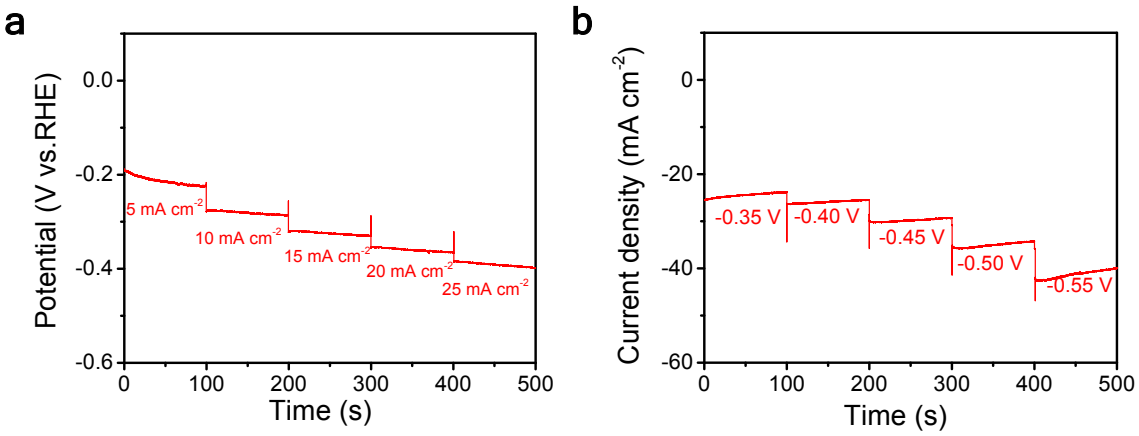

Figure S6. (a) Multi-current step curve of ternary $MoSe_xS_{2-x}$ nanosheets. (b) Multi-potential step curve of ternary $MoSe_xS_{2-x}$ nanosheets.

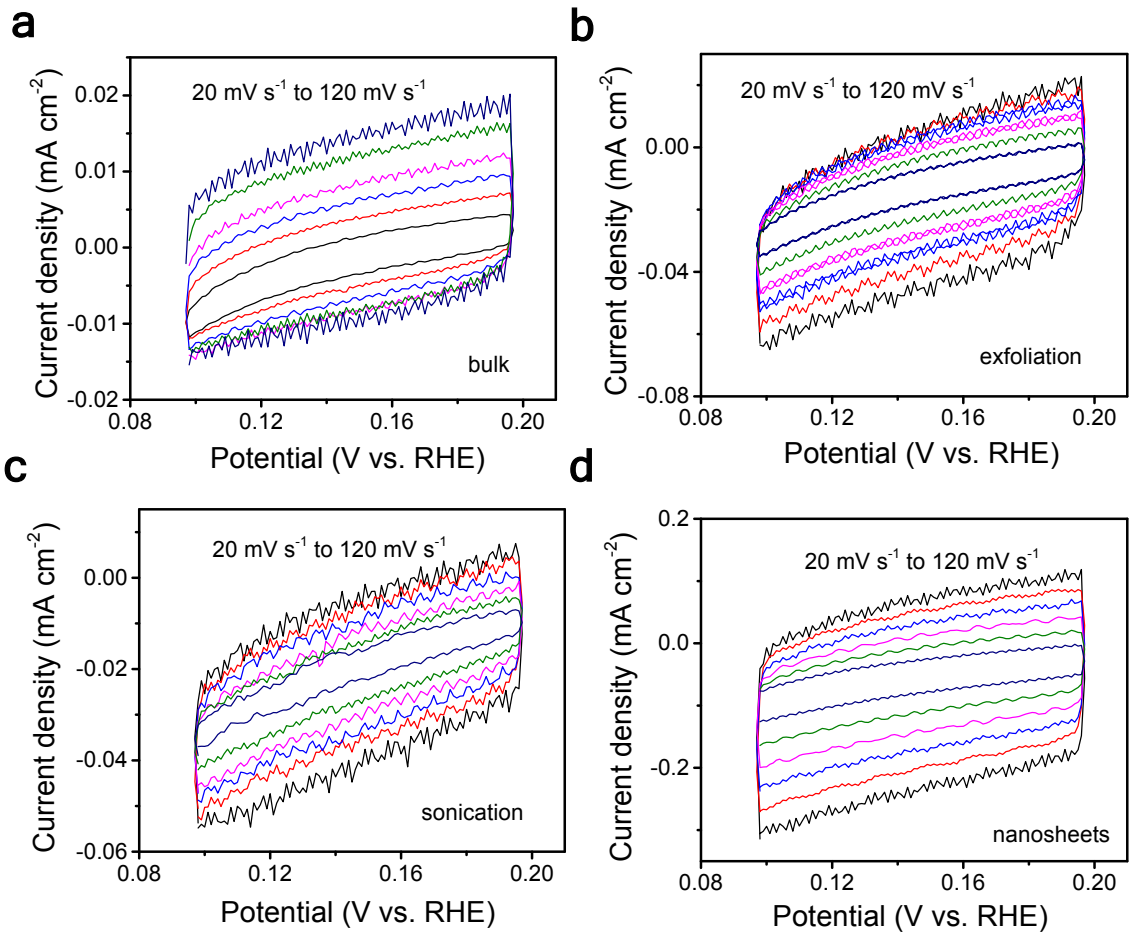

Figure S7. CV curves of (a) bulk $MoSe_xS_{2-x}$, (b) exfoliation $MoSe_xS_{2-x}$, (c) sonication $MoSe_xS_{2-x}$, and (d) ternary $MoSe_xS_{2-x}$ nanosheets.

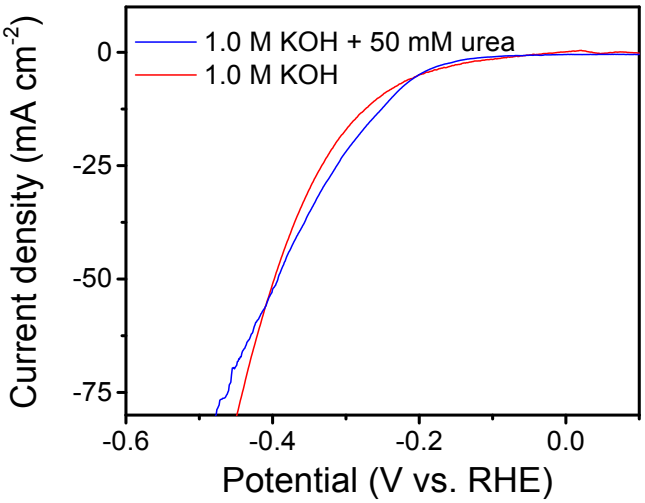

Figure S8. Polarization curves of ternary $MoSe_xS_{2-x}$ nanosheets in 1.0 KOH with and without 50 mM urea.

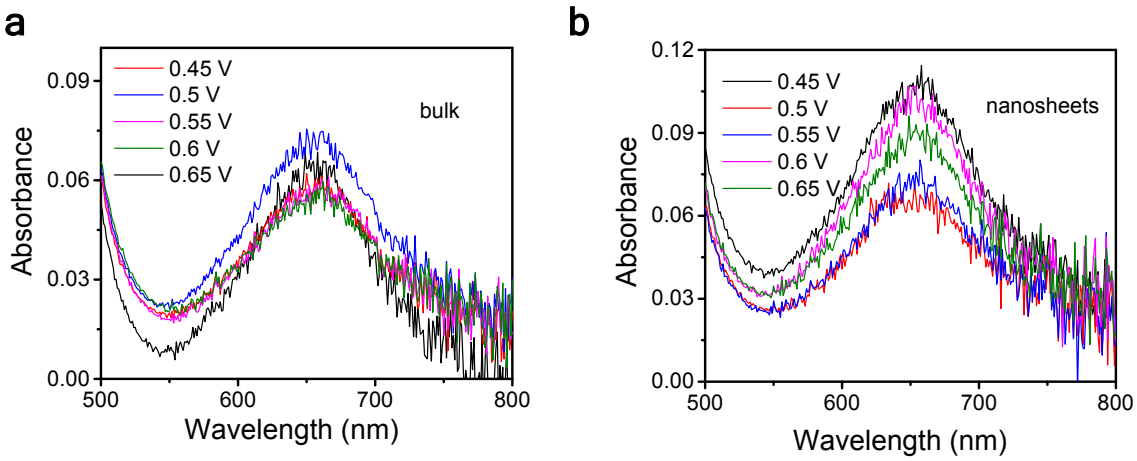

Figure S9. UV-Vis absorption spectra of electrolytes stained with indophenol indicator for 2 h. (a) bulk $MoSe_xS_{2-x}$ and (b) ternary $MoSe_xS_{2-x}$ nanosheets.

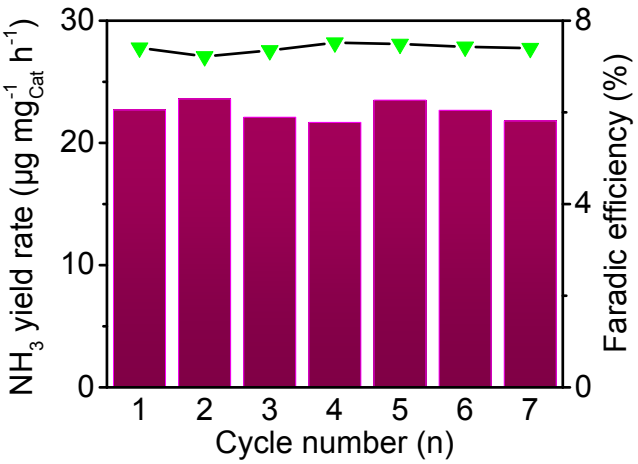

Figure S10. Cycling test of ternary $MoSe_xS_{2-x}$ nanosheets at -0.45 V.

Table S1. Comparison of HER performance of ternary $MoSe_xS_{2-x}$ nanosheets with other reported MoS_2 based materials.

References	Catalyst	Current density (J)	Potential at the corresponding	Electrolyte	Catalyst loading (mg/cm^2)
This work	**$MoSe_xS_{2-x}$/Ni**	**10 mA cm^{-2}**	**123 mV**	**1.0 M KOH**	**0.285**
This work	**$MoSe_xS_{2-x}$ nanosheets**	**10 mA cm^{-2}**	**248 mV**	**1.0 M KOH**	**0.285**
J. Mater. Chem. A, 2016, 4, 18060[1]	$MoSe_{0.94}S_{1.06}$/ CC	10 mA cm^{-2}	183 mV	0.5 M H_2SO_4	0.16
Adv. Funct. Mater. 2018, *28*, 1800852[2]	Mo-thiolate films	10 mA cm^{-2}	294 mV	0.5 M H_2SO_4	N/A
Adv. Funct. Mater. 2017, 27, 1702300[3]	Mo-N/C@MoS_2	10 mA cm^{-2}	117mV	1.0 M KOH	N/A
ACS Catal. 2013, 3, 166[4]	Ni-Mo nanopowder	10 mA cm^{-2}	80 mV	0.5 M H_2SO_4	3
Adv. Energy Mater. 2018, 8, 1801345[5]	1T-2H MoS_2	10 mA cm^{-2}	320 mV	1.0 M KOH	N/A
ACS Catal. 2018, 8, 9529[6]	$Mo_{0.5}W_{0.5}S_2$	10 mA cm^{-2}	138 mV	0.5 M H_2SO_4	0.2

Adv. Funct. Mater. 2018, 28, 1802744[7]	MoS_2-GNR	10 mA cm^{-2}	205 mV	0.5 M H_2SO_4	0.375
Nano Energy 2017, 39, 409[8]	L-Co/MoS_2	10 mA cm^{-2}	156 mV	0.5 M H_2SO_4	0.14

Table S2. Impedance parameters derived from the equivalent circuit model of ternary $MoSe_xS_{2-x}$ nanosheets.

Sample electrode	R_s/Ω	R_{ct}/Ω
bulk $MoSe_xS_{2-x}$	7.742	7,175
sonication $MoSe_xS_{2-x}$	8.174	1,106
exfoliation $MoSe_xS_{2-x}$	9.279	1,370
ternary $MoSe_xS_{2-x}$ nanosheets	9.689	198

Table S3. Comparison of NRR performance of ternary $MoSe_xS_{2-x}$ nanosheets with other reported NRR electrocatalysts

References	Catalyst	Potential (V vs RHE)	NH_3 yield	FE (%)	Electrolyte
This work	**$MoSe_xS_{2-x}$ nanosheets**	**-0.45**	**22.7×10^{-10} mol s^{-1} cm^{-2}**	**7.14**	**0.1 M KOH**
J. Mater. Chem. A, 2018, 6, 3211[9]	Rh nanosheets	-0.2	23.88 μg h^{-1} mg^{-1}	0.217	0.1 M KOH
ACS Appl. Mater. Interfaces, 2018, 10, 28251[10]	TiO_2 nanosheet arrays	-0.7	9.16×10^{-11} mol s^{-1} cm^{-2}	2.5	0.1 M Na_2SO_4
J. Mater. Chem. A, 2018, 6, 24031[11]	$Ti_3C_2T_x$ nanosheets	-0.4	20.4 μg h^{-1} mg^{-1}	9.3	0.1 M HCl
Adv. Mater., 2018, 30, 1803694[12]	Mo_2C/C	-0.3	11.3 μg h^{-1} mg^{-1}	7.8	0.5 M Li_2SO_4
ACS Sustain. Chem. Eng., 2018, 6, 9550[13]	MoN nanosheets	-0.3	3.01 × 10–10 mol s^{-1} cm^{-2}	1.15	0.1 M HCl

References

1. X. Chen, Z. Wang, Y. Qiu, J. Zhang, G. Liu, W. Zheng, W. Feng, W. Cao, P. Hu, W. Hu, *J. Mater. Chem. A,* 2016, **4**, 18060-18066.

2. C. MacIsaac, J. R. Schneider, R. G. Closser, T. R. Hellstern, D. S. Bergsman, J. Park, Y. Liu, R. Sinclair, S. F. Bent, *Adv. Funct. Mater.* 2018, **28**, 1800852.

3. I. S. Amiinu, Z. Pu, X. Liu, K. A. Owusu, H. G. R. Monestel, F. O. Boakye, H. Zhang, S. Mu, *Adv. Funct. Mater.* 2017, **27**, 1702300.

4. J. R. McKone, B. F. Sadtler, C. A. Werlang, N. S. Lewis, H. B. Gray, *ACS Catal.* 2013, **3**, 166-169.

5. S. Wang, D. Zhang, B. Li, C. Zhang, Z. Du, H. Yin, X. Bi, S. Yang, *Adv. Energy Mater.* 2018, **8**, 1801345.

6. H. Wang, L. Ouyang, G. Zou, C. Sun, J. Hu, X. Xiao, L. Gao, *ACS Catal.* 2018, **8**, 9529-9536.

7. J. Ekspong, R. Sandström, L. P. Rajukumar, M. Terrones, T. Wågberg, E. E. Gracia, *Adv. Funct. Mater.* 2018, **28**, 1802744.

8. X. Hai, W. Zhou, S. Wang, H. Pang, K. Chang, F. Ichihara, J. Ye, *Nano Energy* 2017, **39**, 409-417.

9. H. M. Liu, S. H. Han, Y. Zhao, Y. Y. Zhu, X. L. Tian, J. H. Zeng, J. X. Jiang, B. Y. Xia, Y. Chen, *J. Mater. Chem. A,* 2018, **6**, 3211-3217.

10. R. Zhang, X. Ren, X. Shi, F. Xie, B. Zheng, X. Guo, X. Sun, *ACS Appl. Mater. Interfaces* 2018, **10**, 28251-28255.

11. J. Zhao, L. Zhang, X. Y. Xie, X. Li, Y. Ma, Q. Liu, W. H. Fang, X. Shi, G. Cui, X. Sun, *J. Mater. Chem. A,* 2018, **6**, 24031-24035.

12. H. Cheng, L. X. Ding, G. F. Chen, L. Zhang, J. Xue, H. Wang, *Adv. Mater.* 2018, **30**, 1803694.

13. L. Zhang, X. Ji, X. Ren, Y. Luo, X. Shi, A. M. Asiri, B. Zheng, X. Sun, *ACS Sustain. Chem. Eng.,* 2018, **6**, 9550-9554.